Non-coding RNA Research 9 (2024) 732–743

Contents lists available at ScienceDirect

Non-coding RNA Research

journal homepage: www.keaipublishing.com/en/journals/non-coding-rna-research

Original Research Article

MicroRNA-mediated epigenetic regulation of HDAC8 and HDAC6: Functional significance in cervical cancer

Debasmita Naik, Arunasree M. Kalle *

Department of Animal Biology, School of Life Sciences, University of Hyderabad, Hyderabad, Telangana State, 500046, India

ARTICLE INFO

Keywords:
HDAC8
HDAC6
MiRNA
MiR-324–3p
MiR-497–3p
Cervical cancer

ABSTRACT

Cervical cancer, a leading global cause of female mortality, exhibits diverse molecular aberrations influencing gene expression and signaling pathways. Epigenetic factors, including histone deacetylases (HDACs) such as HDAC8 and HDAC6, along with microRNAs (miRNAs), play pivotal roles in cervical cancer progression. Recent investigations have unveiled miRNAs as potential regulators of HDACs, offering a promising therapeutic avenue. This study employed in-silico miRNA prediction, qRT-PCR co-expression studies, and Dual-Luciferase reporter assays to identify miRNAs governing HDAC8 and HDAC6 in HeLa, cervical cancer cells. Results pinpointed miR-497–3p and miR-324–3p as novel negative regulators of HDAC8 and HDAC6, respectively. Functional assays demonstrated that miR-497–3p overexpression in HeLa cells suppressed HDAC8, leading to increased acetylation of downstream targets p53 and α-tubulin. Similarly, miR-324–3p overexpression inhibited HDAC6 mRNA and protein expression, enhancing acetylation of Hsp90 and α-tubulin. Notably, inhibiting HDAC8 via miRNA overexpression correlated with reduced cell viability, diminished epithelial-to-mesenchymal transition (EMT), and increased microtubule bundle formation in HeLa cells. In conclusion, miR-497–3p and miR-324–3p emerge as novel negative regulators of HDAC8 and HDAC6, respectively, with potential therapeutic implications. Elevated expression of these miRNAs in cervical cancer cells holds promise for inhibiting metastasis, offering a targeted approach for intervention in cervical malignancy.

1. Introduction

Cervical cancer poses a significant health burden, ranking as the fourth most prevalent malignancy in developing nations, particularly in countries like India. Its incidence and mortality rates among women are escalating, and contributed to 7.5% of all cancer cases in 2020, as reported by the International Agency for Research on Cancer (IARC). Despite being preventable and treatable through effective screening and vaccination, the disease remains a formidable challenge in economically disadvantaged regions, necessitating urgent preventive interventions [1]. The complexity of cervical cancer treatment is compounded by the disease's stage-dependent therapeutic strategies, with late-stage presentations posing formidable health risks and challenges due to widespread metastasis, often culminating in fatal outcomes.

Microtubules, composed of tubulin polymers, represent ubiquitous cytoskeletal structures crucial for regulating diverse cellular functions, including growth, division, motility, intracellular transportation, organelle placement, and signal transduction [2–5]. In the context of cancer, the dynamic instability of microtubules is intricately linked to processes such as cell proliferation and invasion, positioning them as potential targets for cancer therapeutics [6,7]. Notably, the anticancer agent Paclitaxel functions as a cytoskeletal inhibitor by disrupting tubulin polymerization.

Epigenetic regulation of tubulin through acetylation and deacetylation is a pivotal cellular mechanism influencing microtubule stability and, consequently, cancer dissemination. Histone deacetylases (HDACs), key epigenetic histone modifiers, control alpha-tubulin by reversing lysine acetylation, inducing dynamic microtubule instability. While HDAC6, a class IIb HDAC, has been recognized as a significant regulator of alpha-tubulin [8–12], our research has identified HDAC8 of class I as an additional contributor to alpha-tubulin deacetylation in cervical cancer [13].

RNA interference (RNAi), another epigenetic regulator, plays a crucial role in gene regulation, including the suppression or silencing of specific genes or their messenger RNA (mRNA) products [14,15]. MicroRNAs (miRNAs), a subset of non-coding RNAs, emerge as key players in fine-tuning gene expression and responding to physiological and environmental signals. MiRNAs, by targeting the 3′ untranslated

* Corresponding author.
E-mail address: arunasreemk@uohyd.ac.in (A.M. Kalle).

https://doi.org/10.1016/j.ncrna.2024.02.009
Received 28 November 2023; Received in revised form 25 January 2024; Accepted 17 February 2024
Available online 27 February 2024

region (UTR) of mRNA, guide the RNA-induced silencing complex (RISC) to the target mRNA [16]. Their ability to regulate HDACs underscores their involvement directly and indirectly in the intricate epigenetic and gene expression regulatory network within cells. While limited research has implicated miRNA-mediated HDAC6 regulation in cervical cancer [17], our study aimed to address the notable gap by investigating miRNA-mediated HDAC8 regulation, given its identified oncogenic role in cervical cancer [13]. The primary objective of the current study is to identify a tumor-suppressive miRNA targeting HDAC8, elucidating its capacity to suppress HDAC8 expression and impact on cervical cancer tumorigenesis. Understanding these intricate molecular connections is imperative for unravelling the mechanisms underlying cervical cancer and devising innovative therapeutic strategies.

2. Materials & methods

2.1. Materials

Dulbecco's Modified Eagle's Medium (DMEM), Roswell Park Memorial Institute 1640 (RPMI 1640), Fetal Bovine Serum (FBS), and 100X Anti-Anti (Penicillin-Streptomycin) were procured from Gibco used for cell culture. The 3-(4,5-dimethyl-2-thiazolyl)-2,5-diphenyl-2H-tetrazolium bromide (MTT) was obtained from Himedia used in cell proliferation assay, TRizol from Invitrogen was used for RNA extraction. E. coli poly-A-Polymerase (NEB#MO276), cDNA synthesis kit (TaKaRa Bio#6110A), and Biorad iTaqTM Universal SYBR® Green supermix (172–5120) were used to check relative RNA expression and required primers utilized were procured from Consice Services.

Antibodies used in this study included GAPDH (SC32233), β- Actin (SC1616-R), HDAC6 (SC11420), Vimentin (SC6260), E-cadherin (SC8426), acetylated p53, acetylated HSP90 from Santa Cruz, HDAC8 (Ab187139) from Abcam, α Tubulin (T5168), and Ac-α Tubulin (T6793). FluoroshieldTM with DAPI (F6057) was obtained from Sigma, and Alexa Fluor-488-green was sourced from Invitrogen used in immunofluorescence.

For molecular cloning, enzymes were acquired from Thermo Scientifics: *Sal*I (ER0641), *Xba*I (ER0682), *Bam*HI (ER0055), and T4 DNA ligase (EL0011). Macherey-Nagel™ NucleoSpin™ Gel and PCR Clean-up Kit were utilized for DNA purification. Lipofectamine 3000 from ThermoFisher (L3000001) facilitated efficient transfection, while the Dual-Luciferase assay kit (Promega, E1910) was employed for luciferase activity measurements. The use of these high-quality reagents ensured the reliability and reproducibility of experimental outcomes.

2.2. Methods

2.2.1. Integrated prediction of miRNAs targeting HDAC8 and HDAC6

To identify potential miRNAs targeting HDAC8 and HDAC6, a comprehensive approach was employed using three widely recognized tools: miRDB (http://mirdb.org/), Targetscan7.2 (http://www.targetscan.org/), and miRmap (https://mirmap.ezlab.org/). This integrated strategy, guided by established methodologies [18,19], involved the use of TBtool software for analysis and visualization. TBtool facilitated the identification of overlapping miRNAs from the three prediction databases, addressing the challenge posed by the substantial number of predicted miRNAs across these platforms [20]. A Venn diagram generated with TBtool depicted the common target genes shared by miRNAs across these databases.

The selected miRNAs were further assessed for seed region preference conservation and efficiency, prioritizing canonical sites over non-canonical sites [21–24]. Gibbs free energy (ΔG) calculations were performed using mfold software [25] to assess the stability and authenticity of miRNA-mRNA binding.

Subsequently, the expression levels of the identified miRNAs across various human cancers were determined using miRCancer and the dbDMEC 2.0 database. The predicted miRNAs and their roles in different signaling pathways were analyzed through miRnalyze and the DIANA-miRPath V3.0 database.

Additionally, UALCAN software (http://ualcan.path.uab.edu/) was utilized to analyze tumor subgroup gene expression and the survival of miRNA and mRNA [26,27]. The entire process is schematically depicted in Fig. 1, illustrating the stepwise integration of various computational tools and databases for a comprehensive exploration of miRNA regulation of HDAC8 and HDAC6 in cervical cancer.

2.2.2. Cell culture

The HeLa (Human cervical cancer), HEK293T (Human embryonic kidney), and K562 (Human chronic myelogenous leukemia) cell lines were sourced from the National Centre for Cell Science (NCCS), Pune, India. Upon acquisition, HeLa and HEK293T cells were cultured in Dulbecco's Modified Eagle's Medium (DMEM), while K562 cells were cultured in the RPMI medium. Both media were supplemented with 10% fetal bovine serum and 1% penicillin-streptomycin, all purchased from Gibco, ThermoFisher. Cell maintenance involved incubation in a humidified atmosphere at 37 °C with 5% CO2 to ensure optimal growth conditions.

2.2.3. RNA extraction and quantitative reverse transcription PCR (qRT-PCR) evaluation

Total RNA extraction was carried out using the TRIzol reagent. Following DNaseI treatment, 1 μg of total RNA was reverse transcribed using a cDNA synthesis kit (Takara). E. coli poly(A) polymerase (NEB) was employed to append a Poly-A tail to the miRNA, followed by cDNA

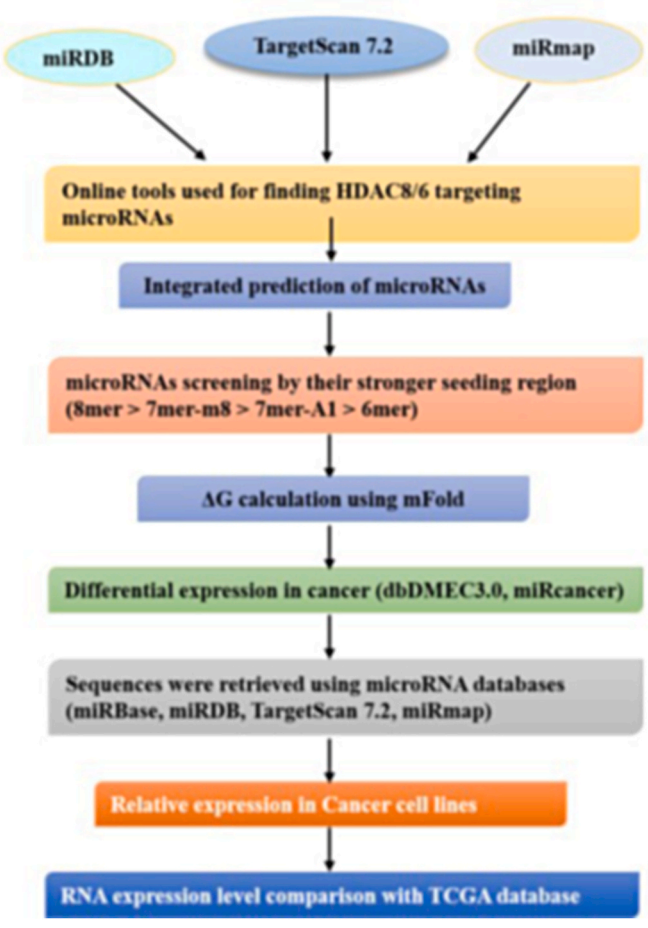

Fig. 1. Schematic representation of methodology used for identifying miRNAs targeting HDAC8 and HDAC6.

synthesis using a universal adaptor primer incorporating oligo-dT [28].

The generated cDNA served as the template for real-time PCR (qRT-PCR) analysis of gene expression using Biorad iTaqTM Universal SYBR® Green supermix and Bio-Rad CFX96 equipment according to the manufacturer's instructions. All primers were custom synthesized by Concise Services (Hyderabad, India) and are detailed in Table 1 β-Actin and U6 snRNA were employed as internal references for mRNA and miRNA detection, respectively, to normalize gene expression results. The $2^{-\Delta\Delta Ct}$ method was applied for comparative quantification, following established protocols [13]. Each sample was used in triplicates in two independent experiments, ensuring robustness and reproducibility of the results.

2.2.4. Protein isolation and western blotting

For Western blot analysis, cellular lysis was conducted using 1X RIPA buffer (50 mM Tris-HCl, 5 mM EDTA, 250 mM NaCl, 50 mM NaF, 0.5 mM Sodium orthovanadate, and 0.5% Triton X-100), supplemented with protease (1X) and phosphatase (1X) inhibitor cocktail (Roche, Sigma). Protein lysates were isolated following a previously established protocol [13], and quantified using the Bradford reagent (Sigma).).

Subsequently, 20–50 μg of protein was separated through 10% or 12% SDS-PAGE and transferred onto a nitrocellulose (NC) membrane. Immunoblot analysis was conducted using primary antibodies against HDAC8, HDAC6, GAPDH, β-actin, α-tubulin, acetylated-α-tubulin, p53, acetyl-Lysine, HSP90, E-Cadherin, and Vimentin. Protein bands were developed and visualized through enhanced chemiluminescence (Roche), and band intensity was quantified using ImageJ 1.34I software (NIH).

2.2.5. Construction of the MiRNA expression plasmids

The precursor miRNA (pre-miR) sequences, encompassing 100 nucleotides on either side of the locus containing *Sal*I and *Bam*HI restriction sites at the 5′ and 3′ ends, were PCR-amplified. Following *Sal*I and *Bam*HI restriction digestion, the pre-miRs were cloned into a pEGFPC1 vector (Fig. 4A) [29,30]. The schematic image for the miRNA expression plasmid is depicted in Fig. 4B.

2.2.6. Luciferase reporter construct

Wild-type (WT) HDAC8 and HDAC6 3′UTR sequences, along with mutant (MUT) sequences harboring altered miRNA binding sites, were PCR-amplified, introducing *Xba*I restriction enzyme sites at both ends (Fig. 4C). After *Xba*I restriction enzyme digestion, the 3′ UTR regions were cloned into a pGL3-promoter vector, resulting in Luciferase reporter vectors [31]. The pGL3-promoter vector devoid of additional nucleotides served as a negative control. The schematic image for the luciferase reporter plasmid is presented in Fig. 4D.

Table 1
Details of primers and oligos used in Real-time expression analysis.

Name of Primer	Sequence (5′-3′)
β-ACTIN FP	CTTGACAAAACCTAACTTGCGC
β-ACTIN RP	GTGAACTTTGGGGGATGCTC
HDAC8 FP	GGCTGCGGAACGGTTTTAAG
HDAC8 RP	GCTTCAATCAAAGAATGCACC
HDAC6 FP	ACCTAATCGTGGGACTGCAAG
HDAC6 RP	GAAAGGACACGCAGCGATCT
U6 FP	GCTTCGGCAGCACATATACTAAAAT
U6 RP	CGCTTCACGAATTTGCGTGTCAT
miR-150–5p FP	TCTCCCAACCCTTGTACCAGTG
miR-664b-3p FP	TTCATTTGCCTCCCAGCCTACA
miR-579–3p FP	TTCATTTGGTATAAACCGCG
miR-497–3p FP	CAAACCACACTGTGGTGTTAGA
miR-26b-3p FP	CCTGTTCTCCATTACTTGGCT
miR-324–3p FP	CACTGCCCCAGGTGCTGCTGG
miR-30b-3p FP	CTGGGAGGTGGATGTTTACTTC
miR-642a-5p FP	GTCCCTCTCCAAATGTGTCTTG
miR-181a-2-3p FP	ACCACTGACCGTTGACTGTACC
miR Universal RP	AAAGCGGCCGCTCTAGTTAGT
Tagged-OligodT	ACTAACTAGAGCGGCCGCTTTTTTTTTTTTTTTTTTTTTTTTTT

2.2.7. Dual luciferase assay

HEK293T cells were seeded at 0.05×10^6 in 24-well plates for investigating miRNA-mRNA interactions. Using Lipofectamine 3000, 60–80% confluent cells were transiently co-transfected with a miRNA expression vector, wild-type/mutant reporter vector, and the pRL-TK vector [31,32](Promega, Madison). Luciferase activity was assessed 24 h post-transfection with an omega FLUOstar microplate reader and the Dual-Luciferase Reporter Assay (Promega, Madison), was normalized using Renilla luciferase activity. Transfections were conducted in triplicate and across three independent experiments.

2.2.8. Transient transfection

HeLa and K562 cells were seeded in 6-well plates at a density of 1.5×10^5 cells per well, reaching 60–80% confluence. Lipofectamine 3000 was utilized to transfect cells with 2 μg of miRNA-expressing plasmid along with an empty vector as the negative control, following the manufacturer's instructions. Transfected media was replaced with regular culture medium 6 h post-transfection, and cells were harvested 48 h later and the RNA and protein isolated were stored at −80 °C and −20 °C, respectively, for future analyses.

2.2.9. Cell viability assay

HeLa cells, plated in 96-well plates with 5000 cells per well one day prior to transfection, were transfected with miRNA expression plasmids using Lipofectamine 3000. The growth medium was replaced with a transfection medium 6 h post-transfection, and cell survival was measured at 24, 48, and 72 h using the MTT assay as per standard protocol [33].

2.2.10. Immunofluorescence

HeLa cells were cultured on coverslips and transfected with the miRNA-expressing plasmid. Subsequently, the cells were fixed in the dark at room temperature (RT) for 15 min using 4% paraformaldehyde. Following two washes with 1X PBS, permeabilization was carried out for 20 min at RT using a 0.5% TritonX-100 solution in 1X PBS. After three additional washes with 1X PBS, cells were blocked for 1 h in a 3% BSA solution in 1X PBST, which included 0.1% TritonX-100. After five more washes with 1X PBS, cells were incubated with α-tubulin-specific primary antibodies at 4 °C overnight. Subsequent to five 1X PBS washes the following day, cells were treated with an Alexa Fluor 488-green secondary antibody for 2 h at 37 °C in the dark, followed by a final set of five 1X PBS washes. Finally, cells were mounted using Fluoroshield mounting medium containing DAPI, and images were captured with a trinocular immunofluorescence microscope (Leica).

2.2.11. Wound healing assay

HeLa cells, cultured to 40–60% confluence in a 6-well plate, underwent miRNA-expressing plasmid transfection, along with an empty vector serving as the negative control. Wounds were generated at three different sites within each well using a 200 μl micro tip. Wound images were acquired using a bright-field microscope at 0 h, 24 h, and 48 h, with wound measurements conducted using ImageJ software.

2.2.12. Statistical analysis

Statistical analyses were performed using GraphPad Prism v6.01 software. Student t-test and one-way analysis of variance (ANOVA) were employed, and statistical significance (p-value) was set at * $\leq$0.05, ** $\leq$0.01, *** $\leq$0.001, **** $\leq$0.0001, and ns = non significance $>$0.05.

3. Results

3.1. Expression of HDAC8 and HDAC6

In our preliminary investigation, we assessed mRNA and protein

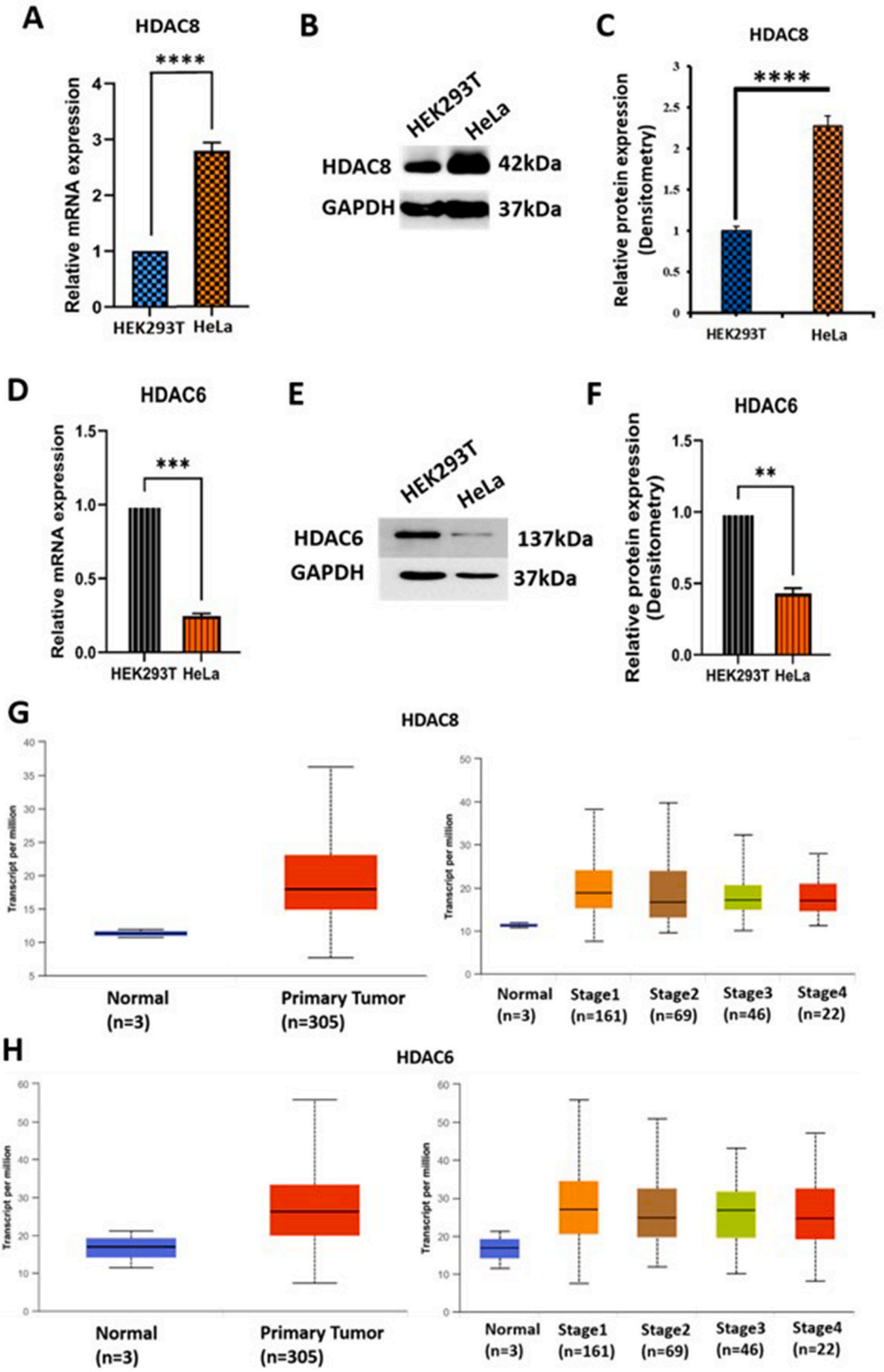

Fig. 2. Expression studies of HDAC8 and HDAC6 in cervical cancer cells: Real-time PCR analysis of HDAC8 (A) and HDAC6 (D) mRNA. Immunoblot showing HDAC8 (B) and HDCA6 (E) protein expression in HeLa cells compared to non-cancerous HEK293T cells. (C) and (F) Densitometry graph of the bands in immunoblots (B) and (E) respectively normalized with GAPDH. Expression of HDAC8 (G) and HDAC6 (H) transcripts in Cervical cancer primary tumors and stage-specific tumors analyzed from TCGA database. **≤0.01, ***≤0.001, and **** ≤0.0001.

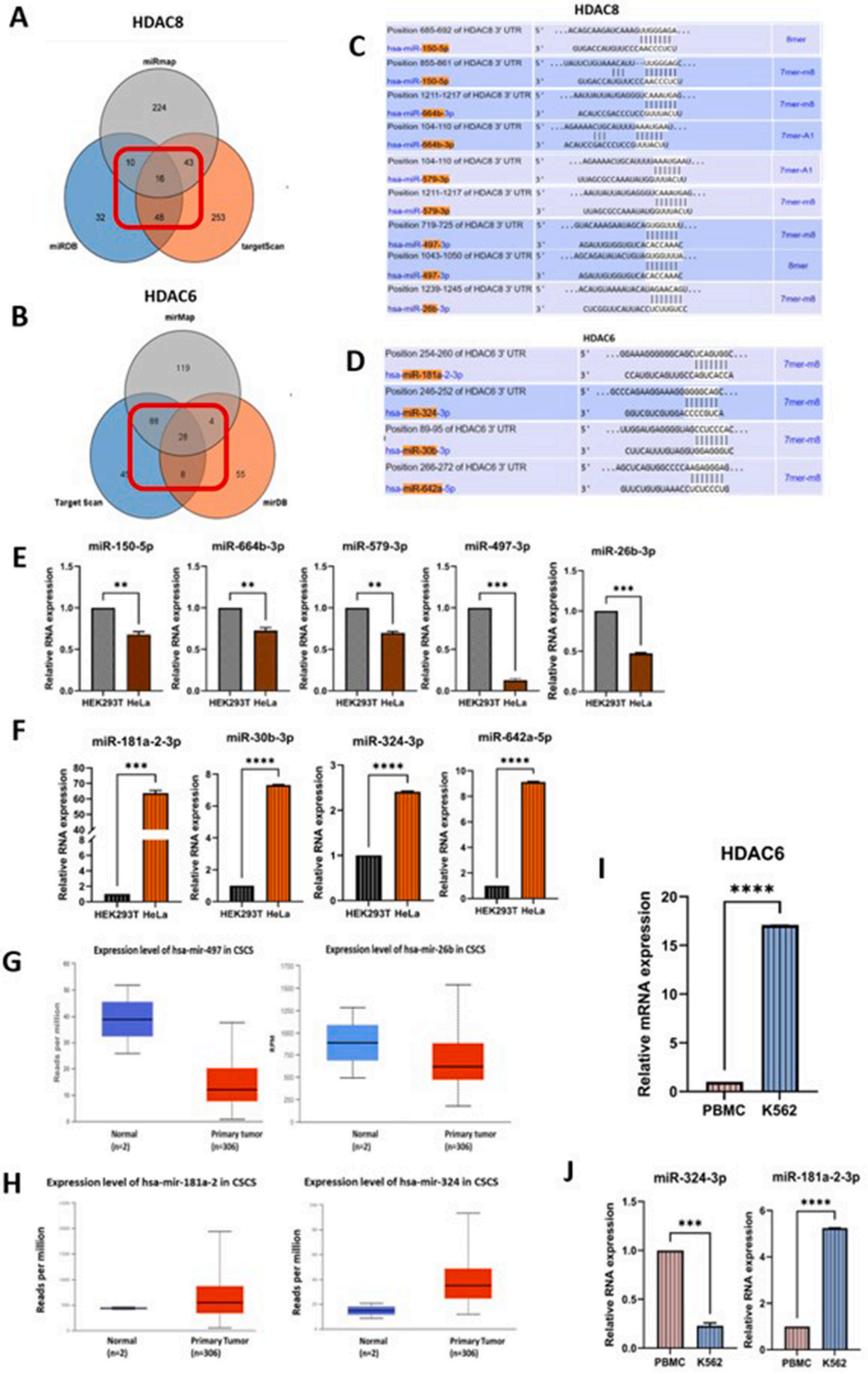

Fig. 3. Integral prediction and expression analysis of HDAC8 & HDAC6 targeting miRNAs in HeLa cells: TBtool software visualization of miRNAs from TargetScan, miRDB, and miRmap software targeting HDAC8 (A) and HDAC6 (B) Details of selected five miRNAs for HDAC8 (C) and four miRNAs for HDAC6 (D) for further validation. Real-time analysis of HDAC8 targeting (E) and HDAC6-targeting (F) miRNAs expression compared to HEK293T cells. Expression of HDAC8-miRNA (G) and HDAC6-miRNA (H) in cervical primary tumor from TCGA database. Real-time analysis of HDAC6 mRNA (I) and miRNA expressions targeting HDAC6 in K562 compared to PBMC cells (J). ** ≤0.01, *** ≤0.001, **** ≤0.0001.

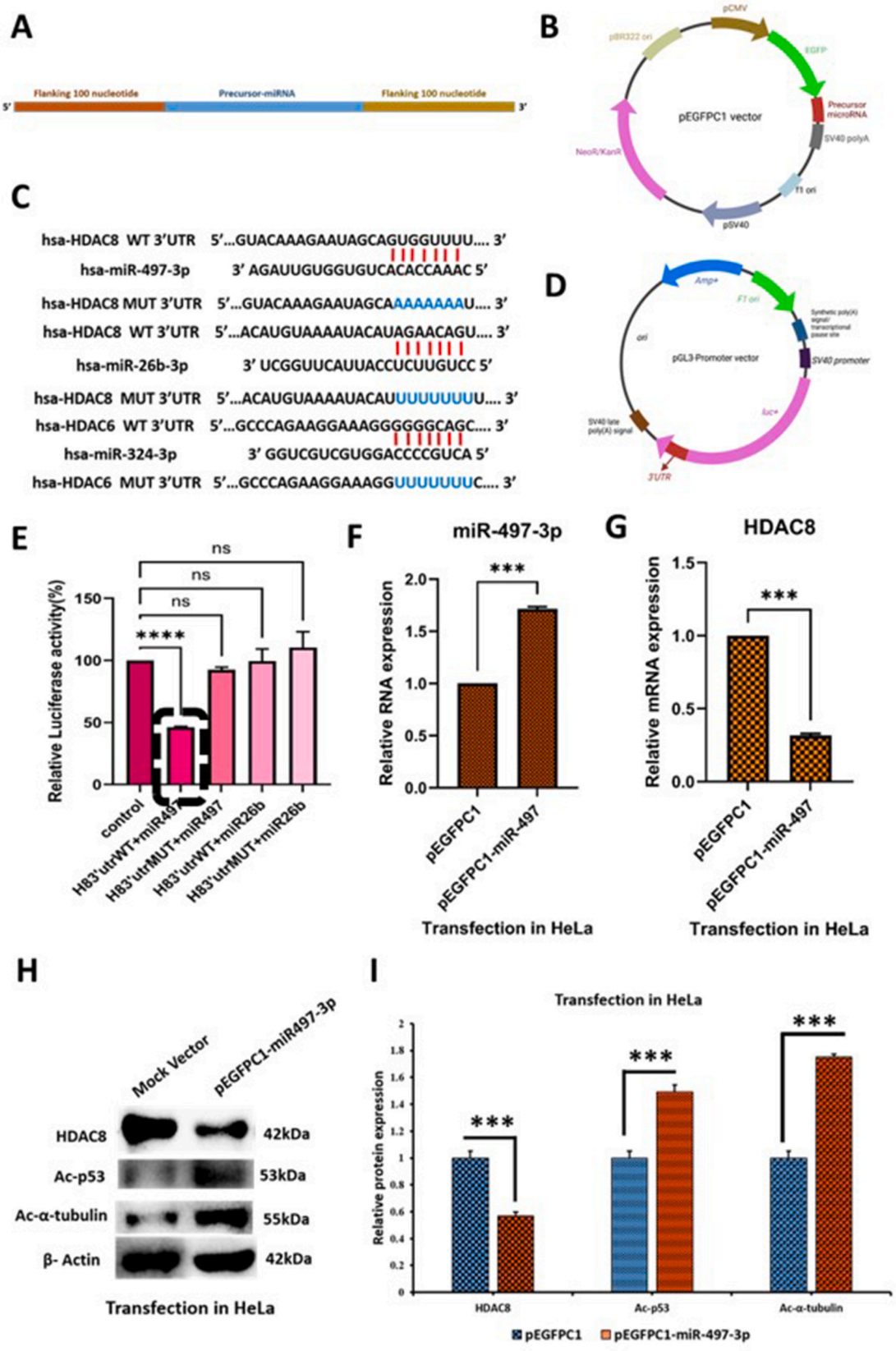

Fig. 4. Validation of miR-497-3p-HDAC8 interaction: Schematic representation of precursor miRNA with flanking nucleotides (A) used in the construction of miRNA expression plasmid with pEGFPC1 plasmid (B). Schematic representation of miRNA binding sequences along with mutation (C) used in the construction of luciferase constructs with pGL3-Promoter vector (D). Dual luciferase assay showing the interaction between miR-497–3p and HDAC8 (E). Real-time analysis shows the expression of miR-497–3p (F) and HDAC8 mRNA (G). Immunoblot shows a protein expression of HDAC8 and its targets acetylated p53 and α-tubulin (H), Densitometry analysis of immunoblot (I). *** ≤0.001, **** ≤0.0001, and ns = non significance >0.05.

expression levels of HDAC8 and HDAC6 in cervical cancer cell line HeLa. Comparative to the non-cancerous HEK293T cell line, HDAC8 exhibited pronounced overexpression in HeLa (Fig. 2A, B, & 2C). In contrast, HDAC6 expression was comparatively low in HeLa cells compared to HEK293T cells (Fig. 2D, E & 2F). Furthermore, TCGA samples revealed significantly high HDAC8 expression in cervical primary tumors and stage-specific tumors (Fig. 2G), while HDAC6 exhibited slightly elevated expression (Fig. 2H).

3.2. MicroRNAs potentially targeting 3′UTR of HDAC8 and HDAC6 mRNA

Employing miRDB, TargetScan, and miRmap, we identified candidate miRNAs targeting the 3′UTR region of both HDAC8 and HDAC6 mRNA. TBtool software visualized the intersection genes of these target genes [20] (Fig. 3A and B). This tool facilitated cluster identification and extraction, emphasizing genes present in multiple databases. Overlapping miRNAs, selected to avoid overlooking potential information, were chosen based on their presence in two or more databases.

Furthermore, miRNAs were scrutinized for canonical binding, emphasizing stronger binding sites that significantly impact repression efficacy. Canonical site classes, including 8mer (binding site complement to 2–8 position of miRNA seed region with an A opposite to 1 position), 7mer-m8 (binding site match 2–8 position of miRNA seed region), and 7mer-A1 (binding site complement to 2–7 position of seed region with an A at opposite one position) [21–23], were prioritized due to potent seed match characteristics [34]. Weaker canonical site types, 6mer (2–7 seed regions match) and offset-6mer (position 3–8 match), were not considered.

MiRNAs with 8mer and 7mer-m8 sites, exhibiting lower ΔG values by mfold software, were further analyzed for their involvement in female-specific cancers through databases like miRcancer and dbDMEC. Consequently, miR-150–5p, miR-664b-3p, miR-579–3p, miR-497–3p, and miR-26b-3p were identified as potential mature miRNAs targeting HDAC8 mRNA (Fig. 3C). Similarly, miR-181a-2-3p, miR-30b-3p, miR-324–3p, and miR-642a-5p were identified as putative miRNAs targeting HDAC6 (Fig. 3D).

3.3. Expression of miRNAs targeting HDAC8 and HDAC6 in cervical cancer cell line

Real-time PCR was employed to assess the expression of five selected potential HDAC8-targeting miRNAs and four HDAC6-targeting miRNAs in HeLa cells compared to HEK293T cells (Fig. 3E and F). All five HDAC8-targeting miRNAs exhibited decreased expression levels, with miR-497–3p and miR-26b-3p showing notably lower expression in HeLa cells, indicating a negative correlation with increased HDAC8 expression. Similar results were observed in cervical TCGA samples for miR-497–3p and miR-26b-3p (Fig. 3G). Consequently, miR-497–3p and miR-26b-3p were chosen for further confirmation. In contrast to HDAC8, all four miRNAs targeting HDAC6 exhibited increased expression levels that negatively correlated with HDAC6 expression, with similar results observed in cervical TCGA samples for miR-181a-2-3p and miR-324–3p (Fig. 3H). Additionally, the K562 cell line, known for its elevated HDAC6 levels, was included in future investigations and notably, HDAC6 mRNA expression in K562 cells surpassed that in PBMCs, as reported in Protein Atlas data (Fig. 3I). Further, the expression analysis in HDAC6-overexpressed K562 cells identified miR-181a-2-3p as a potential candidate for further confirmation (Fig. 3J).

3.4. HDAC8 is a direct target of miR-497–3p

Dual luciferase reporter assays confirmed the direct interaction between HDAC8 and miR-497–3p (Fig. 4A–D). Co-transfection of miR-497–3p with wild-type HDAC8 3′UTR into HEK293T cells resulted in a significant decrease in luciferase activity, validating the interaction (Fig. 4E). Overexpression of miR-497–3p in HeLa cells led to a significant decrease in HDAC8 mRNA and protein levels, resulting in increased acetylation of HDAC8 target proteins, p53, and alpha-tubulin (Fig. 4F, G, 4H, and 4I).

3.5. HDAC6 is a direct target of miR-324–3p

Similarly, dual luciferase reporter assays confirmed the direct interaction between HDAC6 and miR-324–3p. Co-transfection of miR-324–3p with wild-type HDAC6 3′UTR into HEK293T cells resulted in a significant decrease in luciferase activity, confirming the direct interaction (Fig. 5A). Overexpression of miR-324–3p in K562 cells led to a significant decrease in HDAC6 mRNA and protein levels, resulting in increased acetylation of Hsp90 and alpha-tubulin, the client proteins of HDAC6 (Fig. 5B, C, 5D, and 5E).

3.6. Functional significance of miR-497–3p in cervical cancer cell

Functional assays revealed that miR-497–3p overexpression in HeLa cells significantly reduced cell proliferation, induced tubulin polymerization, and inhibited epithelial-mesenchymal transition (EMT). MTT assay demonstrated reduced cell proliferation (Fig. 6A). Immunofluorescence revealed the formation of tubulin bundles in HeLa cells following miR-497–3p transfection (Fig. 6B), confirming tubulin stabilization. Wound-healing assay demonstrated inhibited cell migration (Fig. 6C and D), and Western blot analysis showed decreased expression of the mesenchymal marker Vimentin and increased expression of the epithelial marker E-cadherin, confirming the regulatory role of miR-497–3p in HDAC8-mediated processes (Fig. 6E and F).

4. Discussion

Cervical cancer, the second leading cause of female-specific cancer-related mortality, necessitates a deeper understanding of regulatory mechanisms for effective therapeutic interventions. Epigenetic modulators, such as HDACs and miRNAs, have emerged as crucial players in cancer progression, offering potential avenues for targeted interventions. Our study focused on elucidating the differential expression of HDAC8 and HDAC6, both implicated in cancer progression.

HDAC8, a well-established class I histone deacetylase (HDAC) and X-linked gene, has been extensively implicated in the progression of various cancers, including breast, cervix, lung, liver, and colon [13, 35–40]. Notably, HDAC8 has also been associated with the enhancement of cancer metastasis [41–43]. HDAC6, a member of the class IIb HDAC family, and also an X-linked gene, plays a pivotal role in maintaining cellular homeostasis. Its known function involves the regulation of α-tubulin, crucial for preserving normal cell structure and the cell cycle, as elucidated in previous studies [9].

Contrary to the established role of HDAC6 as a tubulin deacetylase, our previous findings highlighted HDAC8 as the predominant α-tubulin deacetylase in cervical cancer [13], emphasizing the need for understanding the differential regulation of HDAC6 and HDAC8 in cervical cancer cells. MiRNAs have gained prominence as regulators of HDACs in various cancers. So, our hypothesis centered on miRNA-based regulation of HDAC8 and HDAC6 in cervical cancer, seeking novel insights into their regulation.

Our study unveils the nuanced regulatory interplay of microRNAs (miRNAs) in the context of human cervical cancer, with a particular focus on their differential impact on two alpha tubulin deacetylases, HDAC8 and HDAC6. The key findings highlight the distinctive role of miR-497–3p, shedding light on its expression patterns, clinical relevance, and diverse functions in cervical cancer. Our results demonstrate a significant downregulation of miR-497–3p in HeLa cells, concomitant with a marked increase in HDAC8 gene expression when compared to the normal HEK293T cells. This dysregulation suggests a pivotal role for miR-497–3p as a regulator of HDAC8 in cervical cancer. While existing

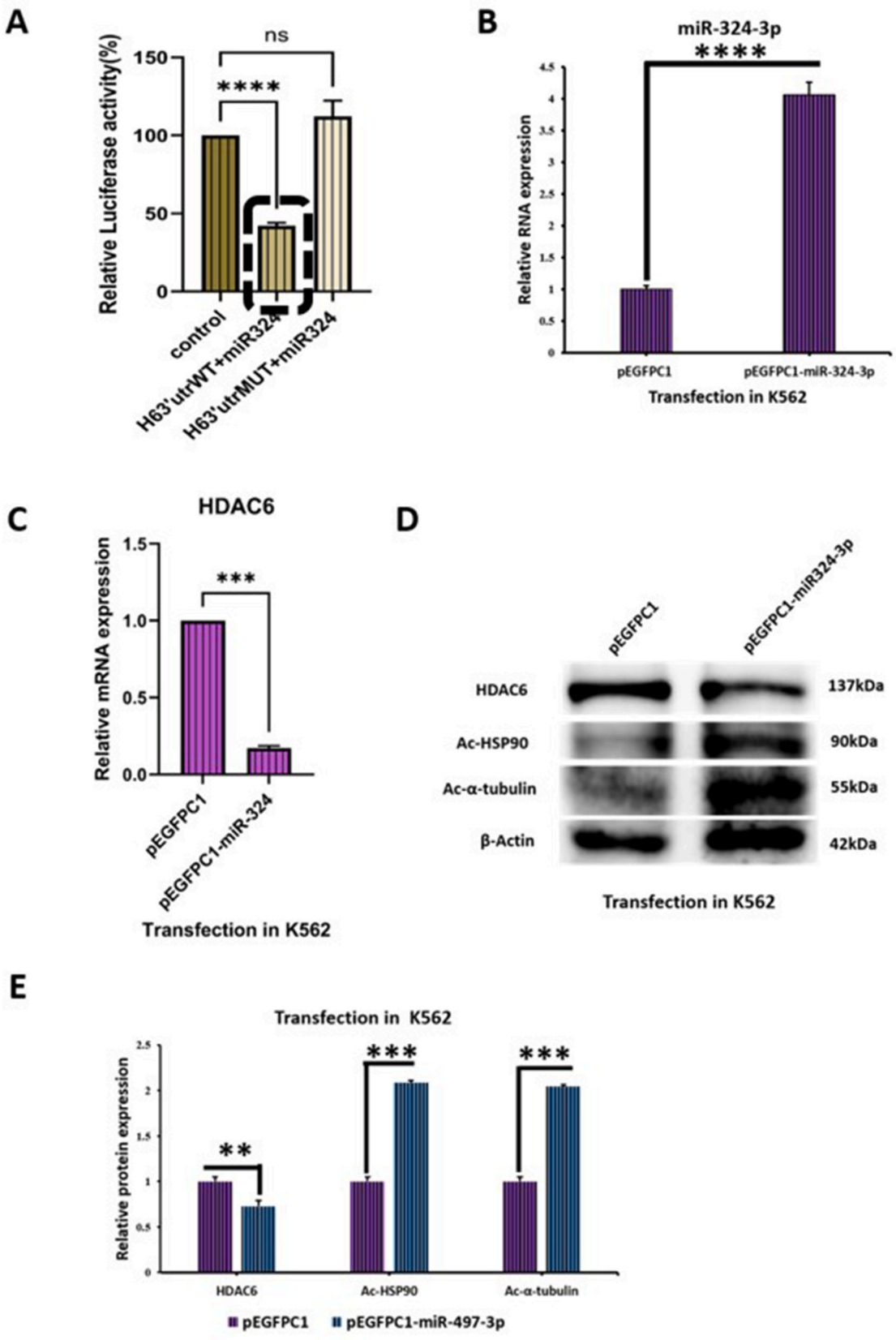

Fig. 5. Over-expression of miR-324–3p suppresses HDAC6: Dual luciferase assay showing the interaction between miR-324–3p and HDAC6 (A). Real-time analysis for expression of miR-324–3p (B) and HDAC6 (C). Immunoblot analysis for expression of HDAC6 and its targets acetylated HSP90 and α-tubulin (D). Densitometry of the immunoblots in D (E). ** ≤0.01, *** ≤0.001, **** ≤0.0001, and ns = non significance >0.05.

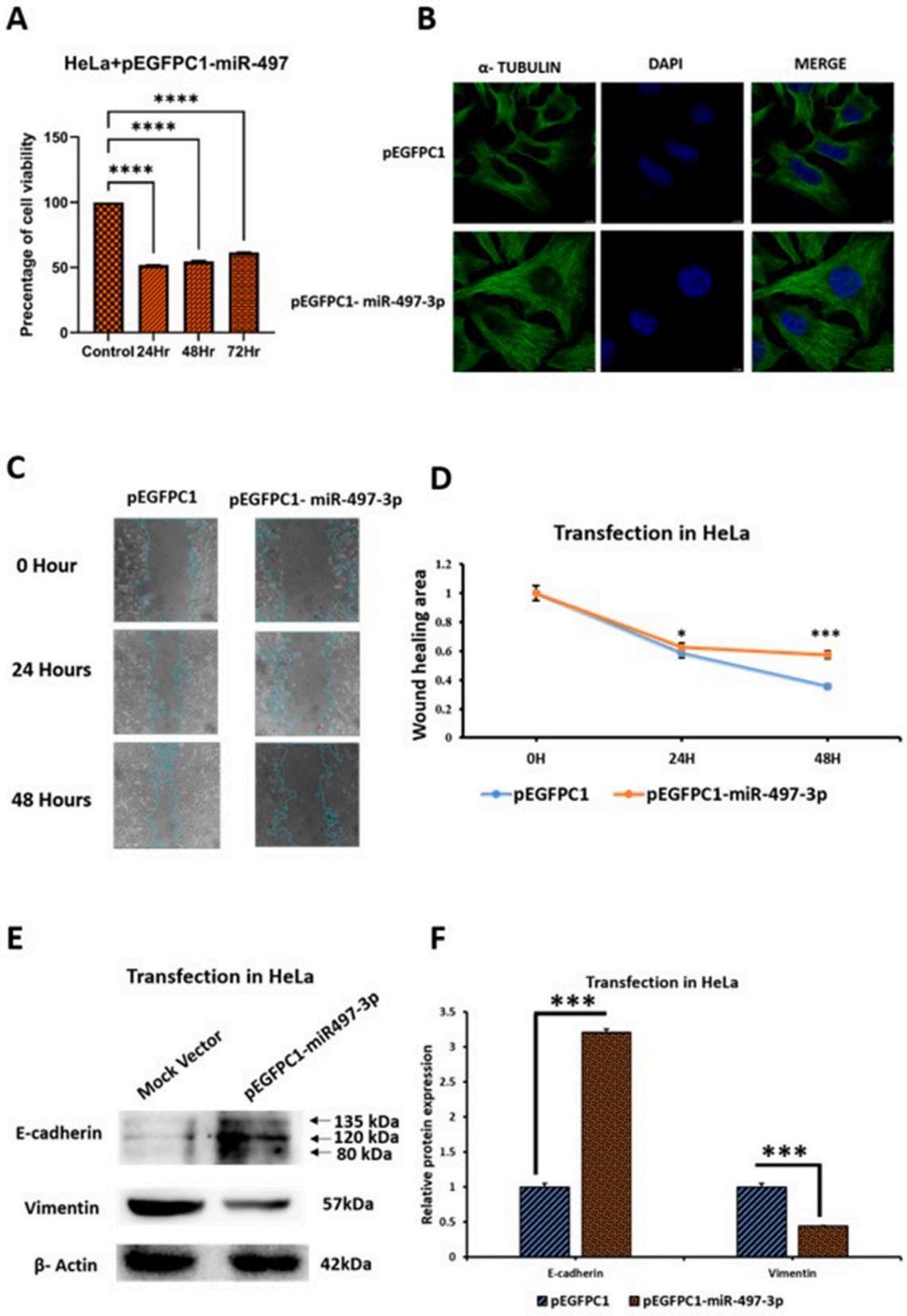

Fig. 6. Over-expression of miR-497–3p suppresses proliferation and metastasis in HeLa cells: cell viability checked through MTT assay for 24, 48, and 72 h (A). Immunofluorescence showing microtubule bundle formation (B). Image shows wound healing assay at 0, 24, and 48 h-time points (C). Graphical representation of wound healing assay (D). Immunoblot showing expression of EMT markers E-cadherin and Vimentin (E). Densitometry of the immunoblots (F). *≤0.05, *** ≤0.001, and **** ≤0.0001.

studies predominantly focus on miR-497–5p in cervical cancer, our research underscores the importance of distinguishing between miRNA isoforms. Unlike miR-497–5p, which is generally acknowledged as a tumor suppressor with lower expression levels, miR-497–3p exhibits a distinct expression pattern and regulatory function in cervical cancer [44–46]. MiR-497 emerges as a multifaceted player with significant clinical implications. Previous studies establish miR-497–5p as a tumor suppressor, a potential prognostic marker, a biomarker [47,48], and a regulator of cisplatin chemosensitivity [49]. The current study expands this repertoire, revealing additional roles for miR-497–3p in various cancer contexts. Beyond its regulatory impact in cervical cancer, miR-497–3p exhibits diverse roles in other cancer types. It emerges as an inhibitor of breast cancer metastasis through the regulation of epithelial-mesenchymal transition (EMT) [50], a hindrance to ovarian cancer progression by targeting the CLDN4 axis [51], a participant in gefitinib resistance in non-small cell lung (NSCL) cancer [26], and a tumor suppressor in thyroid cancer [52]. This versatility positions miR-497–3p as a central player in cancer biology.

In the intricate landscape of cervical cancer, our study delves into the contrasting expression profiles of HDAC6 and miR-324–3p in HeLa cells in comparison to HEK293T cells. Surprisingly, we observed a lower expression of HDAC6 alongside heightened levels of miR-324–3p in HeLa cells, a phenomenon consistently reflected in the TCGA sample. Contrary to our findings, a study by Shi et al. reported higher expression of miR-324–3p in HeLa cells compared to End/E6E7 cells [53]. This discrepancy emphasizes the complexity of miRNA regulation in cancer and necessitates comprehensive investigations to decipher context-specific roles. Intriguingly, our results align with emerging evidence that positions miR-324–3p as a tumor suppressor in various female-specific cancers, including breast and ovarian cancer [38, 54–59]. These studies collectively highlight the potential multifaceted roles of miR-324–3p across distinct cancer types. The observed downregulation of HDAC6, coupled with the tumor-suppressive attributes of miR-324–3p, prompts intriguing questions about their interplay and impact on cervical cancer biology. The complex regulatory network involving HDAC6 and miR-324–3p in cervical cancer warrants further investigation to unveil the underlying molecular mechanisms and their functional consequences.

5. Conclusions

In summary, our investigation has unravelled the pivotal roles played by miRNAs in orchestrating the intricate dance of histone deacetylases, specifically HDAC8 and HDAC6, within the realm of cervical cancer. At the forefront, miR-497–3p emerges as a potent tumor suppressor, steering HDAC8 regulation to inhibit metastasis in HeLa cells. This regulatory paradigm manifests through the elevation of acetylated p53 expression, fortification of acetylated alpha-tubulin stability, and the concurrent suppression of EMT. Crucially, our study extends its reach to illuminate the nuanced regulatory landscape surrounding HDAC6 in HeLa cells, mediated by miR-324–3p. By delineating the molecular intricacies through dual-luciferase assays and probing the downstream effects in K562 cells, we discerned a landscape of inhibited HDAC6 expression at both mRNA and protein levels. Furthermore, this regulatory cascade reverberates across the cellular milieu, amplifying the acetylation levels of HSP90 and alpha-tubulin. Collectively, our findings provide a comprehensive understanding of miRNA-mediated regulatory mechanisms governing HDAC8 and HDAC6 in cervical cancer (see Fig. 7). This not only deepens our insight into the molecular intricacies of cervical carcinogenesis but also charts a

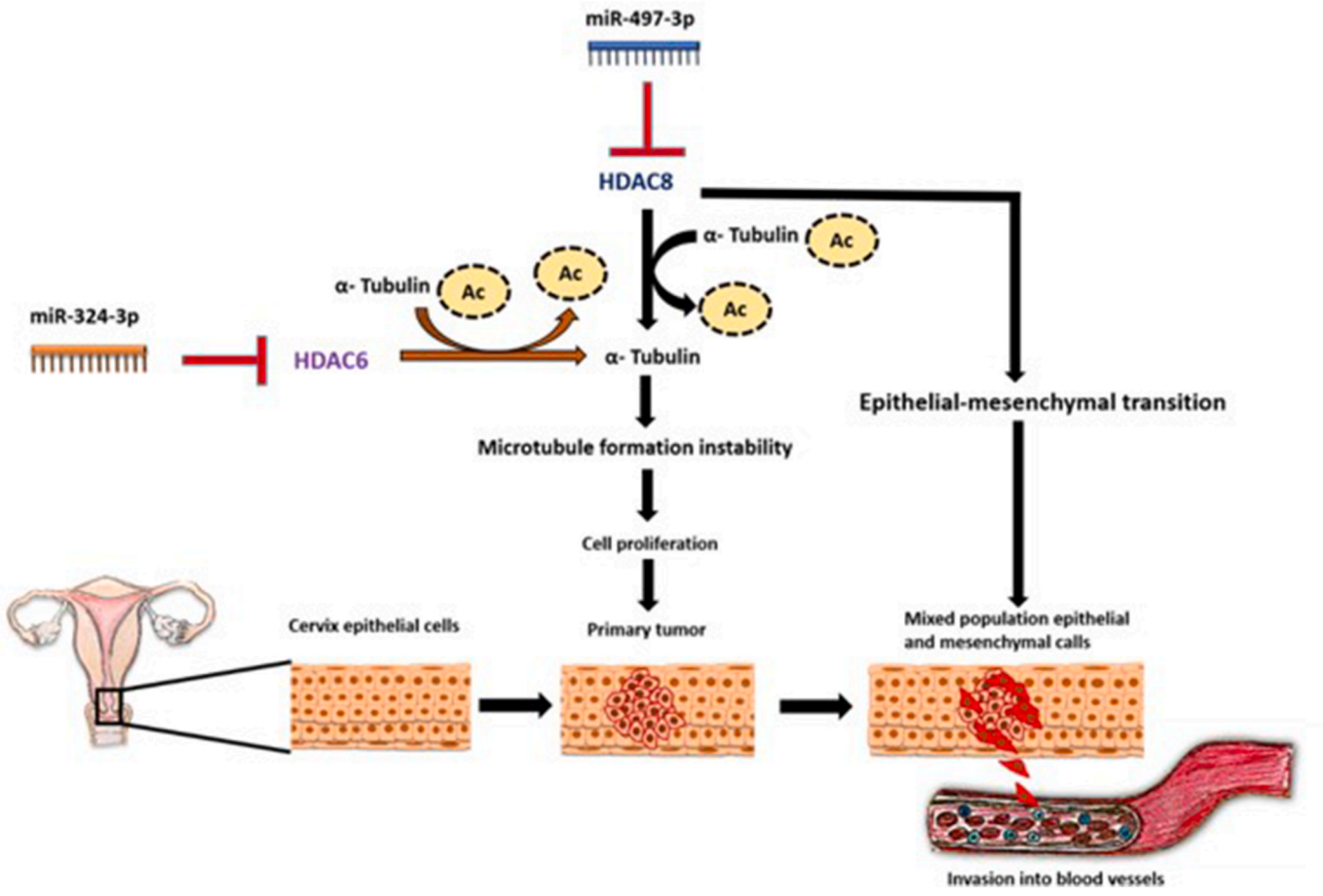

Fig. 7. Schematic diagrams show the overall summary of the study.

promising course toward the development of miRNA-based therapeutic strategies. By identifying miR-497–3p and miR-324–3p as key players in modulating HDAC8 and HDAC6, respectively, our study lays the foundation for future endeavours aiming at precision interventions in the treatment landscape of cervical cancer.

Funding

This work was supported partially by SERB (Grant # EMR/2015/001948), UoH-IoE (Grant# UoH-IoE-RC4-21-016) (A.M.K.) and NMPB (Grant# Z.18017/187/CSS/R&D/TL-01/2021-22-NMPB-IVA) (A.M.K.). DST-FIST (SR/FST/LSI-427/2009 & SR/FST/LSII-041/2015) for infrastructural support to the department. Financial assistance Council of Scientific and Industrial Research Grant#:09/0414 (2015)/2019-EMR-I) (D.N.) is acknowledged.

CRediT authorship contribution statement

Debasmita Naik: Writing – original draft, Investigation, Formal analysis. **Arunasree M. Kalle:** Writing – review & editing, Supervision, Funding acquisition, Conceptualization.

Declaration of competing interest

None.

References

[1] S. Kaur, L.M. Sharma, V. Mishra, M.G.B. Goyal, S. Swasti, A. Talele, P.M. Parikh, Challenges in cervical cancer prevention: real-world scenario in India, South Asian J Cancer 12 (2023) 9–16.
[2] C. Hookway, L. Ding, M.W. Davidson, J.Z. Rappoport, G. Danuser, V.I. Gelfand, Microtubule-dependent transport and dynamics of vimentin intermediate filaments, Mol. Biol. Cell 26 (2015) 1675–1686.
[3] S.L. Prosser, L. Pelletier, Mitotic spindle assembly in animal cells: a fine balancing act, Nature reviews, Molecular cell biology 18 (2017) 187–201.
[4] A. Singh, T. Saha, I. Begemann, A. Ricker, H. Nusse, O. Thorn-Seshold, J. Klingauf, M. Galic, M. Matis, Polarized microtubule dynamics directs cell mechanics and coordinates forces during epithelial morphogenesis, Nat. Cell Biol. 20 (2018) 1126–1133.
[5] G.G. Gundersen, T.A. Cook, Microtubules and signal transduction, Curr. Opin. Cell Biol. 11 (1999) 81–94.
[6] A. Pagano, S. Honore, R. Mohan, R. Berges, A. Akhmanova, D. Braguer, Epothilone B inhibits migration of glioblastoma cells by inducing microtubule catastrophes and affecting EB1 accumulation at microtubule plus ends, Biochem. Pharmacol. 84 (2012) 432–443.
[7] Y. Wu, Y. Zhao, L. Huan, J. Zhao, Y. Zhou, L. Xu, Z. Hu, Y. Liu, Z. Chen, L. Wang, S. Huang, X. He, L. Liang, An LTR retrotransposon-derived long noncoding RNA lncMER52A promotes hepatocellular carcinoma progression by binding p120-catenin, Cancer Res. 80 (2020) 976–987.
[8] A. Matsuyama, T. Shimazu, Y. Sumida, A. Saito, Y. Yoshimatsu, D. Seigneurin-Berny, H. Osada, Y. Komatsu, N. Nishino, S. Khochbin, S. Horinouchi, M. Yoshida, In vivo destabilization of dynamic microtubules by HDAC6-mediated deacetylation, EMBO J. 21 (2002) 6820–6831.
[9] C. Hubbert, A. Guardiola, R. Shao, Y. Kawaguchi, A. Ito, A. Nixon, M. Yoshida, X. F. Wang, T.P. Yao, HDAC6 is a microtubule-associated deacetylase, Nature 417 (2002) 455–458.
[10] Y. Zhang, N. Li, C. Caron, G. Matthias, D. Hess, S. Khochbin, P. Matthias, HDAC-6 interacts with and deacetylates tubulin and microtubules in vivo, EMBO J. 22 (2003) 1168–1179.
[11] J. Asthana, S. Kapoor, R. Mohan, D. Panda, Inhibition of HDAC6 deacetylase activity increases its binding with microtubules and suppresses microtubule dynamic instability in MCF-7 cells, J. Biol. Chem. 288 (2013) 22516–22526.
[12] Y. Li, D. Shin, S.H. Kwon, Histone deacetylase 6 plays a role as a distinct regulator of diverse cellular processes, FEBS J. 280 (2013) 775–793.
[13] G.R. Vanaja, H.G. Ramulu, A.M. Kalle, Overexpressed HDAC8 in cervical cancer cells shows functional redundancy of tubulin deacetylation with HDAC6, Cell Commun. Signal. 16 (2018) 20.
[14] G.K. Barik, O. Sahay, A. Behera, D. Naik, B. Kalita, Keep your eyes peeled for long noncoding RNAs: explaining their boundless role in cancer metastasis, drug resistance, and clinical application, Biochimica et biophysica acta, Reviews on cancer 1876 (2021) 188612.
[15] S. Kodidela, A. Behera, A.B.M. Reddy, Chapter 22 - risk factors and clinical aspects associated with hepatocellular carcinoma: role of long noncoding RNAs, in: G. P. Nagaraju, S. Peela (Eds.), Theranostics and Precision Medicine for the Management of Hepatocellular Carcinoma, Academic Press, Place Published, 2022, pp. 341–356.
[16] D.P. Bartel, MicroRNAs: genomics, biogenesis, mechanism, and function, Cell 116 (2004) 281–297.
[17] W. Wongjampa, T. Ekalaksananan, P. Chopjitt, J. Chuerduangphui, P. Kleebkaow, N. Patarapadungkit, C. Pientong, Suppression of miR-22, a tumor suppressor in cervical cancer, by human papillomavirus 16 E6 via a p53/miR-22/HDAC6 pathway, PLoS One 13 (2018) e0206644.
[18] A. Quillet, C. Saad, G. Ferry, Y. Anouar, N. Vergne, T. Lecroq, C. Dubessy, Improving bioinformatics prediction of microRNA targets by ranks aggregation, Front. Genet. 10 (2019) 1330.
[19] C. Liu, A. Bordeaux, S. Hettich, S. Han, MicroRNA-497-5p functions as a modulator of apoptosis by regulating metadherin in ovarian cancer, Cell Transplant. 29 (2020) 963689719897061.
[20] C. Chen, H. Chen, Y. Zhang, H.R. Thomas, M.H. Frank, Y. He, R. Xia, TBtools: an integrative toolkit developed for interactive analyses of big biological data, Mol. Plant 13 (2020) 1194–1202.
[21] J. Brennecke, A. Stark, R.B. Russell, S.M. Cohen, Principles of microRNA-target recognition, PLoS Biol. 3 (2005) e85.
[22] A. Krek, D. Grun, M.N. Poy, R. Wolf, L. Rosenberg, E.J. Epstein, P. MacMenamin, I. da Piedade, K.C. Gunsalus, M. Stoffel, N. Rajewsky, Combinatorial microRNA target predictions, Nat. Genet. 37 (2005) 495–500.
[23] B.P. Lewis, C.B. Burge, D.P. Bartel, Conserved seed pairing, often flanked by adenosines, indicates that thousands of human genes are microRNA targets, Cell 120 (2005) 15–20.
[24] V. Agarwal, G.W. Bell, J.W. Nam, D.P. Bartel, Predicting effective microRNA target sites in mammalian mRNAs, Elife 4 (2015) e05005.
[25] J. Yue, G. Tigyi, Conservation of miR-15a/16-1 and miR-15b/16-2 clusters, Mammalian genome, official journal of the International Mammalian Genome Society 21 (2010) 88–94.
[26] D.S. Chandrashekar, B. Bashel, S.A.H. Balasubramanya, C.J. Creighton, I. Ponce-Rodriguez, B. Chakravarthi, S. Varambally, UALCAN: a portal for facilitating tumor subgroup gene expression and survival analyses, Neoplasia 19 (2017) 649–658.
[27] D.S. Chandrashekar, S.K. Karthikeyan, P.K. Korla, H. Patel, A.R. Shovon, M. Athar, G.J. Netto, Z.S. Qin, S. Kumar, U. Manne, C.J. Creighton, S. Varambally, UALCAN: an update to the integrated cancer data analysis platform, Neoplasia 25 (2022) 18–27.
[28] R. Shi, Y.H. Sun, X.H. Zhang, V.L. Chiang, Poly(T) adaptor RT-PCR, Methods Mol. Biol. 822 (2012) 53–66.
[29] M.N. Menbari, K. Rahimi, A. Ahmadi, S. Mohammadi-Yeganeh, A. Elyasi, N. Darvishi, V. Hosseini, M. Abdi, miR-483-3p suppresses the proliferation and progression of human triple negative breast cancer cells by targeting the HDAC8>oncogene, J. Cell. Physiol. 235 (2020) 2631–2642.
[30] M. Shafiee, S.A. Aleyasin, M. Vasei, S.S. Semnani, S.J. Mowla, Down-regulatory effects of miR-211 on long non-coding RNA SOX2OT and SOX2 genes in esophageal squamous cell carcinoma, Cell journal 17 (2016) 593–600.
[31] Y. Jin, Z. Chen, X. Liu, X. Zhou, Evaluating the microRNA targeting sites by luciferase reporter gene assay, Methods Mol. Biol. 936 (2013) 117–127.
[32] T. Clement, V. Salone, M. Rederstorff, Dual luciferase gene reporter assays to study miRNA function, Methods Mol. Biol. 1296 (2015) 187–198.
[33] G. Zhao, J.G. Zhang, Y. Liu, Q. Qin, B. Wang, K. Tian, L. Liu, X. Li, Y. Niu, S. C. Deng, C.Y. Wang, miR-148b functions as a tumor suppressor in pancreatic cancer by targeting AMPKα1, Mol. Cancer Therapeut. 12 (2013) 83–93.
[34] D.P. Bartel, MicroRNAs: target recognition and regulatory functions, Cell 136 (2009) 215–233.
[35] T. Dasgupta, J. Antony, A.W. Braithwaite, J.A. Horsfield, HDAC8 inhibition blocks SMC3 deacetylation and delays cell cycle progression without affecting cohesin-dependent transcription in MCF7 cancer cells, J. Biol. Chem. 291 (2016) 12761–12770.
[36] A. Thakur, H. Xu, Y. Wang, A. Bollig, H. Biliran, J.D. Liao, The role of X-linked genes in breast cancer, Breast Cancer Res. Treat. 93 (2005) 135–143.
[37] J.Y. Kim, H. Cho, J. Yoo, G.W. Kim, Y.H. Jeon, S.W. Lee, S.H. Kwon, Pathological role of HDAC8: cancer and beyond, Cells 11 (2022) 3161.
[38] M.C. Ba, Z. Ba, H. Long, S.Z. Cui, Y.F. Gong, Z.F. Yan, K.P. Lin, Y.B. Wu, Y.N. Tu, LncRNA AC093818.1 accelerates gastric cancer metastasis by epigenetically promoting PDK1 expression, Cell Death Dis. 11 (2020) 64.
[39] J. Wu, C. Du, Z. Lv, C. Ding, J. Cheng, H. Xie, L. Zhou, S. Zheng, The up-regulation of histone deacetylase 8 promotes proliferation and inhibits apoptosis in hepatocellular carcinoma, Dig. Dis. Sci. 58 (2013) 3545–3553.
[40] M.N. Menbari, K. Rahimi, A. Ahmadi, A. Elyasi, N. Darvishi, V. Hosseini, S. Mohammadi-Yeganeh, M. Abdi, MiR-216b-5p inhibits cell proliferation in human breast cancer by down-regulating HDAC8 expression, Life Sci. 237 (2019) 116945.
[41] G. Pantelaiou-Prokaki, I. Mieczkowska, G.E. Schmidt, S. Fritzsche, E. Prokakis, J. Gallwas, F. Wegwitz, HDAC8 suppresses the epithelial phenotype and promotes EMT in chemotherapy-treated basal-like breast cancer, Clin. Epigenet. 14 (2022) 7.
[42] J. Chen, L. Cao, J. Ma, C. Yue, D. Zhu, R. An, X. Wang, Y. Guo, B. Gu, HDAC8 promotes liver metastasis of colorectal cancer via inhibition of IRF1 and upregulation of SUCNR1, Oxid. Med. Cell. Longev. 2022 (2022) 2815187.
[43] X. Tang, G. Li, F. Su, Y. Cai, L. Shi, Y. Meng, Z. Liu, J. Sun, M. Wang, M. Qian, Z. Wang, X. Xu, Y.X. Cheng, W.G. Zhu, B. Liu, HDAC8 cooperates with SMAD3/4 complex to suppress SIRT7 and promote cell survival and migration, Nucleic Acids Res. 48 (2020) 2912–2923.
[44] J. Min, D. Jin, F. Zhang, Y. Kang, Y. Qi, P. Du, DLG1-AS1 is activated by MYC and drives the proliferation and migration of hepatocellular carcinoma cells through miR-497-5p/SSRP1 axis, Cancer Cell Int. 21 (2021) 16.

[45] Y. Zhang, X. Li, J. Zhang, L. Mao, E6 hijacks KDM5C/lnc_000231/miR-497-5p/CCNE1 axis to promote cervical cancer progression, J. Cell Mol. Med. 24 (2020) 11422–11433.
[46] Y. Chen, J. Du, Y. Wang, H. Shi, Q. Jiang, Y. Wang, H. Zhang, Y. Wei, W. Xue, Z. Pu, Y. Gao, D. Li, Y. Feng, J. Yan, J. Zhang, MicroRNA-497-5p induces cell cycle arrest of cervical cancer cells in S phase by targeting CBX4, OncoTargets Ther. 12 (2019) 10535–10545.
[47] M. Luo, D. Shen, X. Zhou, X. Chen, W. Wang, MicroRNA-497 is a potential prognostic marker in human cervical cancer and functions as a tumor suppressor by targeting the insulin-like growth factor 1 receptor, Surgery 153 (2013) 836–847.
[48] Y. Zhang, D. Zhang, F. Wang, D. Xu, Y. Guo, W. Cui, Serum miRNAs panel (miR-16-2*, miR-195, miR-2861, miR-497) as novel non-invasive biomarkers for detection of cervical cancer, Sci. Rep. 5 (2015) 17942.
[49] H. Yang, X.L. Wu, K.H. Wu, R. Zhang, L.L. Ju, Y. Ji, Y.W. Zhang, S.L. Xue, Y. X. Zhang, Y.F. Yang, M.M. Yu, MicroRNA-497 regulates cisplatin chemosensitivity of cervical cancer by targeting transketolase, Am. J. Cancer Res. 6 (2016) 2690–2699.
[50] Q. Dong, H. Chen, Y. Li, Y. Kong, C. Geng, Y. Liu, Hsa-miR-497-3p impedes the proliferation and invasion of triple-negative breast cancer cells by controlling epithelial-mesenchymal transition through ZEB1 targeting, Cell Mol Biol (Noisy-le-grand) 69 (2023) 78–83.
[51] Y. Jie, L. Ye, H. Chen, X. Yu, L. Cai, W. He, Y. Fu, ELFN1-AS1 accelerates cell proliferation, invasion and migration via regulating miR-497-3p/CLDN4 axis in ovarian cancer, Bioengineered 11 (2020) 872–882.
[52] Y. Fan, X. Fan, H. Yan, Z. Liu, X. Wang, Q. Yuan, J. Xie, X. Lu, Y. Yang, Hypermethylation of microRNA-497-3p contributes to progression of thyroid cancer through activation of PAK1/β-catenin, Cell biology and toxicology 39 (2023) 1979–1994.
[53] X. Shi, J. Huo, X. Gao, H. Cai, W. Zhu, A newly identified lncRNA H1FX-AS1 targets DACT1 to inhibit cervical cancer via sponging miR-324-3p, Cancer Cell Int. 20 (2020) 358.
[54] N. Zhang, X. Zeng, C. Sun, H. Guo, T. Wang, L. Wei, Y. Zhang, J. Zhao, X. Ma, LncRNA LINC00963 promotes tumorigenesis and radioresistance in breast cancer by sponging miR-324-3p and inducing ACK1 expression, molecular therapy, Nucleic acids 18 (2019) 871–881.
[55] X. Fang, J. Zhang, C. Li, J. Liu, Z. Shi, P. Zhou, Long non-coding RNA SNHG22 facilitates the malignant phenotypes in triple-negative breast cancer via sponging miR-324-3p and upregulating SUDS3, Cancer Cell Int. 20 (2020) 252.
[56] Y. Hou, S. Cai, S. Yu, H. Lin, Metformin induces ferroptosis by targeting miR-324-3p/GPX4 axis in breast cancer, Acta Biochim. Biophys. Sin. 53 (2021) 333–341.
[57] F. Li, Z. Liang, Y. Jia, P. Zhang, K. Ling, Y. Wang, Z. Liang, microRNA-324-3p suppresses the aggressive ovarian cancer by targeting WNK2/RAS pathway, Bioengineered 13 (2022) 12030–12044.
[58] Q.Y. Liu, X.X. Jiang, H.N. Tian, H.L. Guo, H. Guo, Y. Guo, Long non-coding RNA OIP5-AS1 plays an oncogenic role in ovarian cancer through targeting miR-324-3p/NFIB axis, Eur. Rev. Med. Pharmacol. Sci. 24 (2020) 7266–7275.
[59] L. Geng, Z. Wang, Y. Tian, Down-regulation of ZNF252P-AS1 alleviates ovarian cancer progression by binding miR-324-3p to downregulate LY6K, J. Ovarian Res. 15 (2022) 1.